Trends in Phytochemical Research (TPR)

Journal Homepage: https://sanad.iau.ir/journal/tpr

Original Research Article

From plant to nanoparticle: Evaluating the biological efficacy of *Cannabis sativa* L. methanol extract, unlocking the bioapotential of *Cannabis sativa* L. in the green fabrication of silver nanoparticles and their characterization

Majid Mohammadhosseini[1,2*]✉, Behnam Mahdavi[3] And Mohammad Reza Kianasab[1]

[1]Department of Chemistry and Biochemistry, Sha.C., Islamic Azad Uni-versity, Shahrood, Iran
[2]Nanotechnology Research Center, ST.C., Islamic Azad University, Tehran, Iran
[3]Department of Chemistry, Faculty of Science, Hakim Sabzevari University, Sabzevar, Iran

ABSTRACT

Cannabis sativa L. (CSL) is a versatile plant recognized for its medicinal, industrial, and nutritional applications. Rich in bioactive compounds, it has been extensively studied for its phytochemical properties and biological activities. The current report focuses on the preparation of a methanol extract from the stems, flowers, and leaves of this plant, along with an assessment of its relevant biological activities, including antioxidant, antibacterial, and antifungal properties. In the second phase of this study, the green synthesis of Ag nanoparticles was successfully conducted using a methanolic extract of *Cannabis sativa* L. (MECS). In this process, CSL serves as a natural reducing and capping agent. The synthesized nanoparticles were subsequently characterized using Fourier-transform infrared spectroscopy (FT-IR), X-ray diffraction (XRD), energy-dispersive X-ray spectroscopy (EDX), and transmission electron microscopy (TEM). This method offers a sustainable and environmentally-friendly approach to nanoparticle production.

ARTICLE HISTORY

Received: 02 February 2025
Revised: 28 February 2025
Accepted: 03 March 2025
ePublished: 30 March 2025

KEYWORDS

Biological activities
Cannabaceae family
Cannabis sativa L.
Characterization
Green synthesis
Methanol extract
Silver nanoparticles (AgNPS)

1. Introduction

Medicinal and herbal plants play a crucial role in human health due to their diverse array of bioactive natural compounds. These plants have been utilized for thousands of years to treat various health disorders, prevent diseases, and promote overall well-being (Singh et al., 2023; Sharif and Jabeen, 2024). The significance of medicinal plants in sustainable human health management has led to a growing interest in alternative therapies and the therapeutic use of plants (Mohammadhosseini and Jeszka-Skowron, 2023). The main difference between medicinal and narcotic plants lies in their primary effects and regulatory status, rather than their botanical classification. Medicinal plants are used to treat or prevent various health conditions, while narcotic plants contain psychoactive compounds that can alter mental states and are often subject to strict legal controls. However, this distinction is not always clear-cut, as many plants traditionally classified as narcotics also have significant medicinal properties (Arora et al., 2023; Mathur and Ruhm, 2023; Bowe and Kerr, 2024; Lentz et al., 2024). It's important to note that the medicinal value of plants classified as narcotics is increasingly recognized, leading to ongoing debates about their scheduling and regulation (Banerjee et al., 2022). This evolving understanding highlights the complex interplay between a plant's pharmacological properties, its potential for misuse, and its therapeutic applications in modern medicine.

The flowering plant known as *Cannabis sativa* L. (CSL), commonly referred to as *Cannabis*, belongs to the Cannabaceae family and is notable for its diverse applications in medicine, agriculture, and industry (Kianasab et al., 2023). This species has garnered significant attention for its psychoactive and therapeutic properties, primarily due to the cannabinoids it

✉Corresponding author: Majid Mohammadhosseini
Tel: (++98)-23-32394530; Fax: (++98)-23-32394537
E-mail address: majidmohammadhosseini@iau.ac.ir, **https://doi.org/10.71596/tpr.2025.1203169**

produces, such as tetrahydrocannabinol (THC) and cannabidiol (CBD). *Cannabis* has been utilized for thousands of years in both recreational and medicinal contexts, and its popularity has surged recently as scientific evidence substantiates its effectiveness in addressing various health issues, including chronic pain, epilepsy, and anxiety disorders (Kosiba et al., 2019; Wright et al., 2020; Fordjour et al., 2023; Lapierre et al., 2023; Giardina et al., 2024; Ndlovu et al., 2024). In the United States, although *Cannabis* remains illegal under federal law, 38 states have legalized it for medical use, and 24 states have permitted its use for recreational purposes. This trend indicates a significant shift towards greater acceptance and regulation of *Cannabis* (Perlman et al., 2021; Steel et al., 2023). Internationally, countries such as Thailand and Germany are beginning to embrace *Cannabis* legalization; however, challenges persist, particularly in harmonizing state and federal laws (Rehm et al., 2019; Ransing et al., 2022). The chemical composition of CSL is intricate, consisting of over 500 identified compounds, with cannabinoids, terpenes, and flavonoids contributing to its medicinal properties (Kianasab et al., 2023). The Food and Drug Administration (FDA) has approved CBD for specific epilepsy syndromes, while ongoing research aims to explore the plant's potential in combating cancer and its possible applications in health and wellness (Fordjour et al., 2023; Bukowska, 2024). Growing demand for eco-friendly products is prompting growers to adopt sustainable cultivation practices, which, in turn, help reduce their environmental impact (Wilson et al., 2025). The significance of *Cannabis* in culture cannot be overstated; it has been deeply intertwined with social activism, artistic expression, and community development. The evolution of *Cannabis* culture reflects a broader movement toward greater acceptance and normalization, transforming perceptions of *Cannabis* from a stigmatized substance to one that fosters wellness, creativity, and self-identity (Leinen et al., 2023; Matos et al., 2025).

Green synthesis of silver nanoparticles (AgNPs) using plant extracts has emerged as a simple, cost-effective, and environmentally-friendly approach in the field of nanotechnology. This method leverages the reducing and stabilizing properties of various phytochemicals present in plant extracts to convert silver ions into stable AgNPs (Cásedas et al., 2022; Moond et al., 2023). The process typically involves mixing plant extracts with silver nitrate solution, resulting in the reduction of Ag^{+} to Ag^{0} and the subsequent formation of AgNPs (Asif et al., 2022; Pradeep et al., 2022). Plant extracts contain a diverse array of bioactive compounds, including phenolic acids, flavonoids, alkaloids, terpenoids, and proteins, which play crucial roles in the synthesis and stabilization of AgNPs (Pradeep et al., 2022; Moond et al., 2023). These phytochemicals not only facilitate the reduction of silver ions but also act as capping agents, preventing agglomeration and controlling the size and shape of the nanoparticles. The formation of AgNPs is often indicated by a color change in the reaction mixture, typically from light yellow to dark brown, and can be confirmed through various characterization techniques such as UV-visible spectroscopy, X-ray diffraction (XRD), and scanning electron microscopy (SEM) (Meena et al., 2020; Vanlalveni et al., 2021; Asif et al., 2022). The surface plasmon resonance (SPR) peak observed in UV-visible spectra, usually between 400-580 nm, serves as a key indicator of AgNP formation (Meena et al., 2020; Asif et al., 2022). This green synthesis approach offers several advantages over traditional physical and chemical methods, including simplicity, cost-effectiveness, and reduced environmental impact. Moreover, the biogenic AgNPs often exhibit enhanced stability and biocompatibility due to the natural capping agents present in the plant extracts (Vanlalveni et al., 2021). The size, shape, and properties of the synthesized AgNPs can be influenced by various factors, including the type of plant extract, concentration of phytochemicals, pH, temperature, and reaction time (Moond et al., 2023; Velgosova et al., 2024). This versatility allows for the tailoring of AgNPs for specific applications, particularly in the field of antimicrobial agents, where they have shown promising results. As research in this area continues to expand, the green synthesis of AgNPs using plant extracts represents a sustainable and efficient approach to nanoparticle production, with potential applications across various fields including medicine, environmental remediation, and materials science. The ever-evolving *Cannabis* landscape is fraught with disputes regarding its regulation, medical efficacy, and broader social implications, making CSL a significant topic for both scientific inquiry and public discourse.

The primary objective of this study was to explore the biological potential of methanol extracts of *Cannabis sativa* L. (MECS) prepared from its stems, flowers, and leaves and evaluating their antioxidant, antibacterial, and antifungal activities. This research aims to provide a comprehensive assessment of the plant's biological properties, contributing to the growing body of evidence on its therapeutic potential. A secondary but equally significant objective was to develop an eco-friendly approach for the green synthesis of AgNPs using MECS as a reducing and capping agent. The study emphasizes sustainable nanomaterial production while focusing on the detailed characterization of the synthesized AgNPs using Fourier-transform infrared spectroscopy (FT-IR), XRD, energy-dispersive X-ray spectroscopy (EDX), and transmission electron microscopy (TEM) techniques. These objectives aim to combine the fields of phytochemistry and nanotechnology to pave the way for future applications in biomedicine and environmental remediation.

2. Experimental

2.1. Reagents and materials

All chemicals, reagents, standards, and solvents used were of analytical grade and purchased from Merck, unless otherwise specified. HPLC-grade methanol (purity ≥ 99%) was obtained from Sigma-Aldrich. Deionized

water was utilized throughout the experiments. All glassware was thoroughly cleaned with pure acetone and rinsed with deionized water prior to use.

2.2. Plant material: Collection and identification

Samples of the entire plant material (*C. sativa* L.) were collected in May 2024 during the full flowering stage from the mountainous regions of Bandar Torkaman in Golestan Province, located at geographical coordinates 36°54′06″N 54°04′15″E. The necessary permits were obtained from the Anti-Narcotics Police of Golestan Province, Iran, as this plant is classified as a controlled substance. A local botanist initially identified the plant material, and a voucher specimen of a representative sample of CSL was subsequently stored at the herbarium of Semnan Province Agricultural and Natural Resources Research and Education Center (Shahrood) (ANRRECjk).

2.3. Apparatus

In this study, a Sartorius precision balance with an accuracy of 0.0001 g was utilized for weighing the samples. A rotary evaporator (model L-1001WEV) manufactured by Wisd, China, was employed for solvent removal and evaporation. An ultrasonic bath (model Elmasonic P60H) from Elma, Germany, was used to disperse the particles and homogenize the solution. The UV-Vis spectra were recorded using a Shimadzu UV-160A spectrophotometer, which is equipped with deuterium and tungsten lamps and is capable of measuring absorbance in the wavelength range of 200 to 1000 nm.
All infrared (IR) spectra were obtained using a Shimadzu FT-IR spectrometer (model IR-460) in potassium bromide (KBr) pellet form. The XRD patterns of the synthesized nanoparticles were determined using an X-ray diffractometer (STOE, PW2773/00, Germany) with Cu Kα radiation at a wavelength of 1.54 Å. Peak analysis and interpretation were conducted using X'Pert Pro MPD software. Transmission electron microscopy (TEM) was performed using a Philips XL_{30} microscope, which offers high-resolution imaging and high magnification to analyze the structure and morphology of the materials.

2.4. Preparation of methanolic extract from the aerial parts of CSL

Maceration is a straightforward technique commonly used to prepare plant extracts. It involves soaking the plant material in an appropriate solvent for an extended period, which facilitates the release of active compounds into the liquid (Rajasekar et al., 2023; Amalia et al., 2024). This method effectively extracts the desired substances, as the prolonged interaction between the solvent and the plant material enhances the dissolution and diffusion of these compounds. As a practical and cost-effective approach, maceration offers an efficient means of obtaining extracts rich in bioactive compounds, which can be utilized for various applications (Murti et al., 2024; Xiang et al., 2024). After receiving the complete CSL plant from the central warehouse of the Anti-Narcotics Police of Golestan Province, various parts of the plant, including leaves, flowers, and stems, were air-dried in a shaded environment. Following the traditional soaking method for preparing plant extracts, 150-g portions of each part were immersed in sufficient amounts of methanol for three days. To prevent spoilage, the liquid was completely covered with aluminum foil. A laboratory shaker was also utilized to enhance the extraction process. The resulting solution was then filtered twice through filter paper to eliminate any remaining suspended materials. In the final stage, the solution was transferred to a rotary evaporator set at 60 °C under vacuum conditions. After the solvent was removed, a concentrated, tar-like, and sticky extract was obtained, which underwent comprehensive phytochemical analyses.

2.5. Antioxidant activity assays

2.5.1. Free radical scavenging activity (RSA) assay

1,1-Diphenyl-2-picrylhydrazyl (DPPH) is a stable free radical that, in the presence of a hydrogen-donating compound, receives a hydrogen and is reduced to its reduced form. The DPPH radical, due to its strong absorption at 517 nm, has a dark purple color in solution and, in the presence of an electron-donating molecule, is reduced and neutralized, changing to colorless or light yellow. The degree of color reduction of the DPPH solution is proportional to the radical scavenging ability. This reduction occurs through the transfer of a hydrogen atom from the antioxidant molecule to the unpaired electron of the nitrogen atom in DPPH (Mishra et al., 2012). This assay is simple and reproducible and only requires a UV/Vis spectrophotometer to perform, which explains the widespread use of this antioxidant screening method. However, interpretation becomes complicated when compounds have absorption at 517 nm and overlap with DPPH. The color of the compound can be eliminated through other radical or reduction reactions, as well as other irrelevant reactions and the determining factor in this regard is the structure of the presumed compound.
In this study, the radical absorption of the plant extracts (MECS) was measured using the method described by Mahdavi et al. (2022). Initially, 1.5 mL of each extract, at concentrations ranging from 80 to 1000 µg/mL, was combined with 1 mL of a methanolic DPPH solution (0.1 mM). The resulting mixture was kept in the dark at room temperature for 90 minutes, following two minutes of vigorous shaking to ensure complete reaction. The absorbance of the samples was then measured at 517 nm. All measurements were conducted in triplicate, with butylated hydroxytoluene (BHT) used as a synthetic antioxidant standard. The percentage of inhibition of the extracts, which indicates their free radical scavenging ability, was calculated using Eqn. 1:

$$\text{Inhibition } \% = [(A_c - A_s)/A_c] \times 100 \quad \text{(Eqn. 1)}$$

In this equation, A_c and A_s account for the absorbance of

the control (DPPH + methanol) and the sample (DPPH + plant extract), respectively. By examining the trend of changes in the percentage of free radical scavenging (with the sample absorbance available) versus the extract concentration, the inhibitory concentration (IC_{50}) quantity can be calculated. It is evident that a smaller IC_{50} value indicates a greater radical scavenging activity of the extract. By definition, IC_{50} is the minimum concentration of extract required to remove 50% of free DPPH radicals in the reaction environment (Gulcin and Alwasel, 2023).

2.5.2. Total phenolic content (TPC) assay

The determination of total phenolic content (TPC) was conducted using the Folin-Ciocalteu reagent (FCR), which involves several key steps. This procedure, widely accepted in the scientific community, has been extensively validated for its reliability in quantifying total phenolics in various plant extracts and food samples (Blainski et al., 2013; Lawag et al., 2023). Initially, reagents were prepared, including the FCR, a 20% (w/v) sodium carbonate solution, and a gallic acid standard solution (1 mg/mL). A calibration curve was then established using gallic acid standards ranging from 5 to 100 µg/mL. For analysis, 100 µL of each standard or sample was mixed with 4.5 mL of distilled water and 100 µL of FCR. After 3 minutes, 300 µL of Na_2CO_3 (20% *w/v*) solution was added, the resulting mixture was subsequently incubated at room temperature (25 °C) for 90 minutes in dark conditions and the relevant optical density was measured at 765 nm using a UV-Vis spectrophotometer. Sample extracts are typically diluted to 1 mg/mL before analysis. TPC was calculated using the calibration curve ($y = 0.013x + 0.0324$; $R^2 = 0.9966$) and expressed as milligrams of gallic acid equivalents (GAE) per gram of sample (mg GAE/g). The assay should be performed under reduced light due to reagent sensitivity, and pH should be maintained around 10.

2.5.3. Total flavonoid content (TFC) assay

Flavonoids are beneficial antioxidants that have recently gained much attention due to their promising effects in combating diseases (Li et al., 2023). One common method for measuring the total flavonoid content in extracts is the colorimetric method based on the formation of aluminum-flavonoid complexes (Chandra et al., 2014; Ramos et al., 2017; Shraim et al., 2021). The main basis of the TFC assay method is the formation of a stable acid complex with the carbon 4 ketone group and carbon 3 and 5 hydroxyl groups of flavones and flavonols (Ramos et al., 2017; Shraim et al., 2021), as well as an unstable acid complex with ortho-dihydroxyl groups in ring A or B of flavonoids (Shraim et al., 2021). The TFC of the extracts was calculated using the aluminum chloride method and the results were expressed in milligrams per gram of dry extract (mg RuEA g^{-1}). Accordingly, 1 mL of each extract (100 µg/mL) was mixed with 1 mL of methanolic aluminum chloride solution (2.0 *w/w*%). After 30 minutes in darkness at room temperature, the absorbance of the samples was measured at 415 nm. This process was repeated three times for each extract and the standard rutin curve was used for the assessment of TFC of each extract at concentrations of 25, 50, 75, 100, 200, and 300 µg/mL.

2.6. Antimicrobial activity of MECS

2.6.1. Determination of minimum inhibitory concentration (MIC) and minimum bactericidal concentration (MBC)

Quantitative analysis of the minimum inhibitory concentration (MIC) was conducted using the microbial growth method, while the minimum bactericidal concentration (MBC) was determined through the tube dilution method (Torres et al., 2013; Coronado-Aceves et al., 2016). The MIC, defined as the lowest concentration of an extract that can inhibit bacterial growth under laboratory conditions, was evaluated using a 96-well microplate in the broth microdilution assay.

A well containing a bacterial suspension and dimethyl sulfoxide (DMSO) without the extract was used as the positive control to evaluate any potential effects of DMSO on bacterial growth. Additionally, a negative control well containing only nutrient broth and the extract, without the microbial suspension, was included. Each well was filled with 100 µL of nutrient broth, and 100 µL of the plant extract at an initial concentration of 500 mg/mL was added to the first well. Serial dilutions were performed from 250 mg/mL to 25 mg/mL by transferring 100 µL from one well to the next, continuing this process until the last well, from which 100 µL was discarded. Subsequently, 50 µL of the microbial suspension was added to each well and the microplate was incubated at 37 °C for 24 hours. After 24 hours, MIC was determined by measuring turbidity at 630 nm using a UV/Vis spectrophotometer. The well exhibiting the lowest absorbance value was reported as the MIC. Additionally, the well with the lowest concentration of the extract that showed no visible turbidity was identified as the MIC well. The MIC was defined as the lowest concentration that resulted in a 90% reduction in turbidity compared to the control group. To determine the MBC, 5 µL from each concentration was plated onto Mueller-Hinton Agar and incubated for 24 hours at 37 °C. The MBC is defined as the lowest concentration of the extract that is capable of killing 99.9% of the bacterial population.

2.6.2. Antifungal assay method

The procedure for evaluating the antifungal activity of plant extracts is similar to the antibacterial approach, with the fungal strain *Candida albicans* replacing the bacterial strains.

2.7. The procedure for the synthesis of AgNPs using MECS

Over the past decade, the use of MECS in scientific

literature for the green synthesis of nanoparticles has been on an upward trend (Bawazeer et al., 2020; Demarchi et al., 2020; Arabkhani et al., 2022). The method employed for the synthesis of AgNPs is similar to one of the previous works of this research group (Zhang et al., 2021), albeit with some modifications. Initially, a solution containing silver nitrate at a concentration of 1 mM was prepared and heated to a temperature of 70 °C. Subsequently, 2 mL of the plant extract prepared in the earlier stage was added to the solution, which was then heated again at 70 °C for 12 hours. After this period, the solution was allowed to cool to room temperature. In the next step, the cooled solution was centrifuged at 12,000 rpm for 15 minutes at 4 °C. The obtained precipitate was then dried in an oven at 70 °C for 5 hours. The synthesized AgNPs were stored in a microtube at 4 °C for further analysis.

3. Results and Discussion

3.1. Antioxidant activity results

3.1.1. Results of antioxidant assessment of MECS using the DPPH radical scavenging method

In evaluating the antioxidant capacity of MECS prepared from the stems, leaves, and flowers of CSL using the 2,2-diphenyl-1-picrylhydrazyl (DPPH) free radical scavenging assay, the IC_{50} values were determined (µg/mL). Under optimal experimental conditions, the percentage of free radical scavenging was plotted as a function of extract concentration for each plant part and the corresponding linear equations were utilized to calculate the relevant IC_{50} values. Based on these calculations, the IC_{50} values for the MECS stems, flowers, and leaves were found to be 698.01, 315.75, and 590.97 µg/mL, respectively (Fig. 1). As illustrated in Fig. 1, the concentration of methanolic extracts required to inhibit 50% of DPPH free radicals (IC_{50}) was compared to that of BHT. Accordingly, the IC_{50} value for the positive control (BHT) was found to be approximately 11.84 µg/mL, which is significantly lower than the IC_{50} values of the methanolic extracts. A lower IC_{50} value indicates a higher antioxidant capacity. Therefore, the results suggest that the standard antioxidant BHT exhibited significantly greater antioxidant activity than the methanolic extracts from various parts of CSL. As anticipated, the experimental findings demonstrated that increasing the concentration of the extracts resulted in enhanced DPPH radical scavenging activity.

A literature survey indicates that CSL extracts exhibit significant antioxidant activity against DPPH radicals, with IC_{50} values ranging from 60 to 97 µg/mL for aqueous and hexane extracts, respectively (Cásedas et al., 2022). These results are comparable to or even better than those of isolated compounds such as CBD and Δ^9-THC extracts, which demonstrated an IC_{50} of 141.9 µg/mL (Cásedas et al., 2022). In comparison to previous reports, the values obtained in the current study reflect moderate antioxidant activity, which can be attributed to the variability in antioxidant capacity based on several factors, including the characteristics of the sampling area, soil composition, the date of plant collection, the specific plant part used and the extraction method employed. For example, leaf extracts exhibited DPPH radical scavenging activity of 75% at a concentration of 500 µL/mL (Hourfane et al., 2023), while seed extracts showed an IC_{50} of 14.5 mg/mL (Hourfane et al., 2023). The antioxidant activity is likely due to the presence of polyphenols, cannabinoids, and other bioactive compounds in CSL (Cásedas et al., 2022; Hourfane et al., 2023). Interestingly, different varieties of CSL, such as Tygra, have shown superior DPPH radical scavenging activity, with results ranging from 0.92 to 0.93 mg trolox/g of plant material for leaves and inflorescences (Stasiłowicz-Krzemień et al., 2023).

3.1.2. Results of the total phenolic content (TPC) of CSL

The numerical values of TPC for CSL organs viz. flowers, leaves and stems were determined regarding the gallic acid (GA) standard curve (Fig. 2) which have been shown in Table 1. In accordance with the data tabulated in this table, MECS from the leaves and the stems of CSL displayed the most and the least amounts of TPCs, respectively 52.1 and 14.2 mg GAE/g.

It seems rational that TPC of CSL varies significantly depending on the plant part, extraction method, and cultivar. Table 2 demonstrates the significant variations in TPCs across different parts of CSL in several reports. In this context, studies have reported a wide range of values, from as low as 0.44 mg/g in cold-pressed hemp seed oil to as high as 52.58 mg GAE/g in inflorescences. In this sense, in inflorescence samples, TPC ranged from 10.51 to 52.58 mg GAE/g, with free radical-scavenging capacity between 27.5 and 77.6 mmol trolox/kg (Izzo et al., 2020). In a related study, the TPC was determined using a spectrophotometric method at 760 nm, following standard procedures for the construction a calibration curve based on rutin (Motiejauskaitė et al., 2023). Various extraction solvents were tested, with Triton X-100 yielding the highest TPC content at 72.73 mg $RuEg^{-1}$ dry weight, indicating its superior extraction efficiency for phenolic compounds. Methanol (MeOH) extraction followed, providing a TPC of 54.49 mg $RuEg^{-1}$ dry weight, which was significantly lower than that of Triton X-100. In contrast, extraction using water proved to be the least effective, resulting in a TPC of only 12.51 mg $RuEg^{-1}$ dry weight. These results underscore the importance of solvent selection in maximizing the extraction of phenolic compounds from hemp inflorescences (Motiejauskaitė et al., 2023).

More recently, Ahidar et al. (2024) determined the TPC of three different extracts of CSL: hexanic, ethanolic, and chloroformic. The results were expressed as mg of gallic acid equivalent per gram of extract (mg GAE/g ext). In this regard, the hexanic extract exhibited the highest TPC, recorded at 2.225 mg GAE/g ext, indicating a significant concentration of phenolic compounds. The ethanolic extract showed a TPC of 1.938 mg GAE/g ext, which is lower than that of the hexanic extract, remains substantial. The chloroformic extract had the lowest

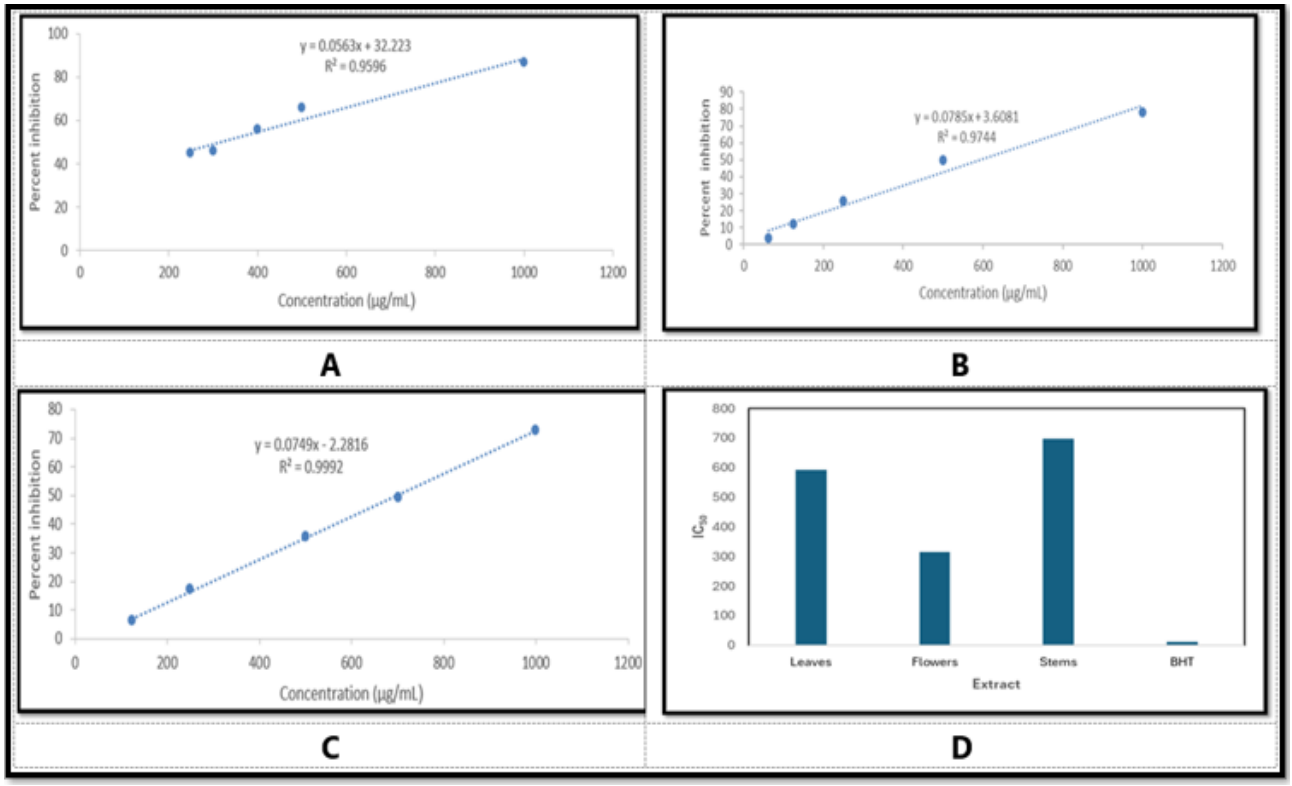

Fig. 1. DPPH radical scavenging activity (%) of *Cannabis sativa* L.: **A:** Flowers, **B:** Leaves, **C:** Stems; **D:** Comparison of the effect of methanolic extracts of *Cannabis sativa* L. and butylated hydroxytoluene (BHT) positive control on DPPH radical inhibition.

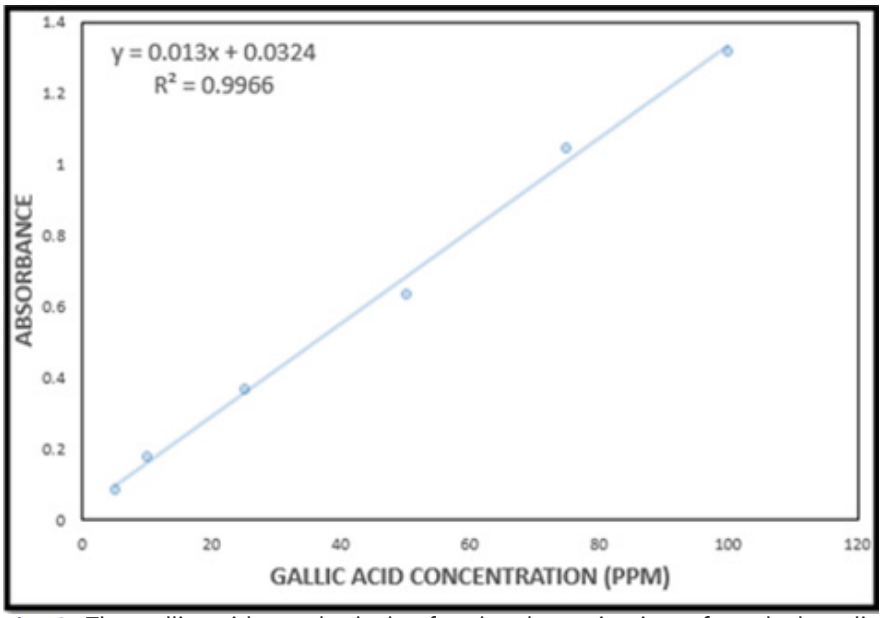

Fig. 2. The gallic acid standard plot for the determination of total phenolic contents (TPCs) of methanol extracts from different organs of *Cannabis sativa* L. (flowers, stems and leaves).

TPC among the three, with a value of 1.802 mg GAE/g ext (see Table 2). These findings suggest again that the choice of extraction solvent plays a crucial role in the solubility and concentration of phenolic compounds, as supported by previous studies. This variation highlights the importance of considering specific plant tissues and extraction techniques when evaluating the phenolic profile of CSL. The simple comparison of our findings with the tabulated TPCs in table clarifies that the TPC value found in our research aligns with the previous

Table 1
Total phenolic contents (TPCs) of methanol extracts of of flowers, stems and leaves of *Cannabis sativa* L. (CSL).

Arial part of *Cannabis sativa* L.	TPC[1] (mg Gallic acid/g sample)
Flowers	24.9 ± 2.8
Stems	14.1 ± 1.8
Leaves	3.3 ± 51.1

[1]TPC: Total phenolic content.

Table 2
The the total phenolic content results of *Cannabis sativa* L. reported in some of the previous works in the literature.

Plant part	Extraction method	TPC range (mg GAE/g)	Cultivar/Region	Notable compounds	Reference
Inflorescence	Polar extraction	10.51 - 52.58 [a]	Kompoti, Tiborszallasi, Antal, Carmagnola Cs	Cannflavin A, B; Quercetin-3-glucoside	Izzo et al., 2020
Aerial parts	Methanol	7.59-23.06 [b]	Greenhouse of Horticultural Sciences, Tabriz, Iran	CBD, Δ9-THC, cannabinoids, chlorophyll a, b; carotenoids	Mirzamohammad et al., 2021
Flowers	Ethanol	1.938	Ketama region, Morocco	Flavonoids, terpenoids, saponins	Ahidar et al., 2024
	Chloroform	1.802			
	Hexane	2.225			
Seeds (oil)	Cold-pressed	1.16 mg	Poland	Not specified	Kalinowska et al., 2022
Inflorescence	Triton X-100 (2.0%)	72.73 [c]	LRCAFEF [d]	Cannabinoids	Motiejauskaitė et al., 2023
	Methanol	54.49 [c]			
	H_2O	12.51[c]			
Leaves	Aqueous ethanol (70%) [e]	12.02-39.49	Shanxiand Hunan of China	Flavonoids, phenolics and cannabinoids	Liu et al., 2022
Leaves and inflorescences	DES [f]	7.76 [g]	South Hemp	Cannabidiol (CBD) and cannabidiolic acid (CBDA	Tiago et al., 2022
			Tecnosrl (Taranto, Puglia)		

[a] The highest total phenols content resulted from *Carmagnola* Cs with the content of 41.517 mg GAE/g and, the lower amount emerges for the Kompolti variety (10.510 mg GAE/g).; [b] Applying different salicylic acid (SA) concentrations as foliar treatment; [c] mg RUE/g; [d] Lithuanian Research Centre for Agriculture and Forestry Experimental Fields; [e] using heat-reflux-extract; [f] Deep Eutectic Solvents; [g] Lactic acid glucose (Lac:Gluc: 5:1).

reports.

3.1.3. Results of the total flavonoid content of CSL

According to the findings of this study, the TFC results from various extracts of CSL, based on the rutin standard calibration curve (Fig. 3), are presented in Table 3. As seen in this table, the lowest and highest flavonoid contents were observed in the stem extract (9.13 ± 1.87 mg RuE/g) and the leaf extract (48.06 ± 1.47 mg RuE/g), respectively.

As indicated in the literature, CSL exhibits a diverse and significant flavonoid profile, with TFCs varying based on plant part, cultivar, and geographical origin. The flavonoids in CSL primarily consist of flavones (*e.g.*, apigenin, luteolin) and flavonols (*e.g.*, kaempferol, quercetin), present both as aglycones and glycosides (Bautista et al., 2021). Notably, CSL produces unique prenylated flavones known as cannflavins (A, B, and C), with cannflavins A and B exhibiting remarkably high concentrations in inflorescences, averaging 61.8 and 84.5 mg/kg, respectively (Izzo et al., 2020). Among the flavonols, quercetin-3-glucoside was particularly abundant, reaching up to 285.9 mg/kg in the *Carmagnola* CS cultivar (Izzo et al., 2020). Flavanols such as catechin and epicatechin were also significant, with mean concentrations of 53.3 and 66.2 mg/kg across cultivars (Izzo et al., 2020). Geographical variations in flavonoid composition have also been observed. For instance, leaves from Sichuan showed higher concentrations of flavonoid-C glycosides and correspondingly higher antioxidant activity, while those

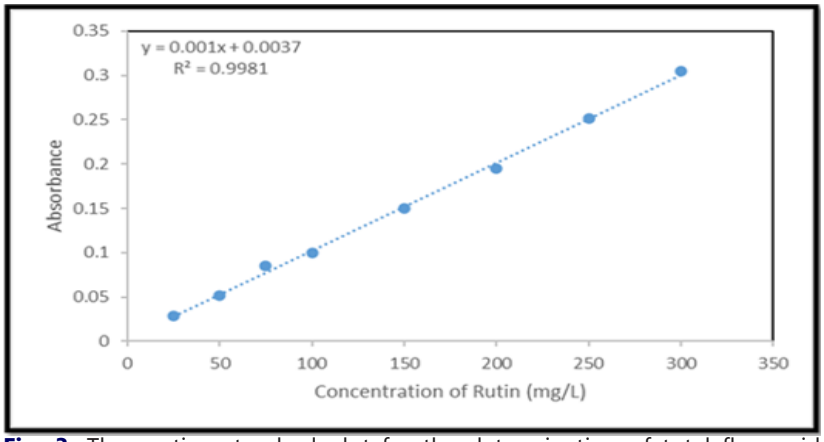

Fig. 3. The routine standard plot for the determination of total flavonoid contents (TFCs) of methanol extracts from different organs of *Cannabis sativa* L. (flowers, stems and leaves).

Table 3
Total flavonoid contents (TFCs) of methanol extracts of flowers, stems and leaves of *Cannabis sativa* L. (CSL).

Arial part of Cannabis sativa L.	TFC[1] (mg Rutin/g sample)
Flowers	18.35 ± 3.1
Stems	9.13 ± 1.9
Leaves	1.5 ± 48.06

[1]TFC: Total flavonoid contents.

from Shaanxi and Xinjiang contained more flavonoid-*O* glycosides and demonstrated slightly lower antioxidant activity (Chen et al., 2024). Environmental factors and cultivation conditions can significantly influence flavonoid accumulation, as evidenced by studies utilizing salicylic acid treatments, which enhanced both total flavonoid content and antioxidant capacity in CSL (Mirzamohammad et al., 2021). The TFC in CSL leaves was estimated to be around 1.0%, consistent with comprehensive profiling studies (Jin et al., 2020). This substantial presence of flavonoids, combined with the unique cannflavins, positions CSL as a potential novel source of polyphenols for nutraceutical applications (Izzo et al., 2020; Chen et al., 2024). An interesting study has investigated cannabinoid biosynthesis in CSL, focusing on polyketide synthase (PKS) activities in plant tissues (Flores-Sanchez and Verpoorte, 2008). In this relation, the TFC in bracts showed significant variation over time, with values of 2.18 mg/100 mg dry weight (DW) at 24 days, decreasing to 0.40 mg/100 mg DW at 31 days for one sample group. In fruits, the flavonoid content was notably low, recorded at 0.06 mg/100 mg DW for one variety and 0.05 mg/100 mg DW for another. Seedlings exhibited higher flavonoid content, ranging from 1.17 to 1.67 mg/100 mg DW across different samples. Female leaves had a higher total flavonoid content compared to male leaves, with values between 2.24 and 2.54 mg/100 mg DW. Male flowers showed the lowest flavonoid content, with values ranging from 0.46 to 0.81 mg/100 mg DW, indicating a significant difference compared to female flowers. The kaempferol content in bracts of the fiber-type variety (Kompolti) was significantly lower than that in drug-type varieties (Skunk and Fourway) at day 31. Quercetin content was highest in male flowers, particularly from fiber-type plants, which showed significant differences compared to drug-type plants (Flores-Sanchez and Verpoorte, 2008). Recently, Ahmad et al. (2019) have assessed the TFC of the crude extracts of CSL using various solvents, with methanol yielding the highest TFC (59.03 mg QE/g). Additionally, ethanol provided significant results, with a TFC of 56.00 mg QE/g. It was also found that the other solvents such as chloroform, acetone, and hexane produced varying results, with chloroform showing minimal TFC values and acetone yielding 12.086 mg QE/g for CSL. The results were presented as mean values with standard deviations, and statistical analysis indicated that the same letters within a column denote no significant difference ($p > 0.05$) according to Duncan's multiple range test. A brief review of the TFC values obtained in the present study aligns with those reported in previous research, indicating consistency among the findings.

3.2. Antimicrobial results

3.2.1. Results of antimicrobial activity assessment for determination of MIC and MBC of MECS

The effects of MECS (500 mg/mL) obtained from the aerial parts of CSL (stems, flowers, and leaves) were evaluated for their ability to inhibit bacterial growth

using the broth dilution method to determine the MIC and MBC. The final MIC and MBC values for the methanolic extracts against the tested bacteria are presented in Table 4, expressed in mg/mL. All experiments were conducted in triplicate and the mean values were reported as the MIC and MBC results. For the aerial parts of MECS, the MIC values were recorded as follows: Flower extract ranged from 0.03 µg/mL to 16 mg/mL, leaf extract ranged from 0.06 to 32 mg/mL, and stem extract ranged from 8 mg/mL to 32 mg/mL.

According to the literature, CSL exhibits significant antimicrobial activity, particularly against Gram-positive bacteria. CBD and other major cannabinoids demonstrate potent effects, with MICs ranging from 1 to 4 µg/mL against various strains of *Staphylococcus aureus*, including methicillin-resistant *S. aureus* (MRSA) (Blaskovich et al., 2021). The MBC for CBD against MRSA was found to be 2 µg/mL, indicating rapid bactericidal activity (Blaskovich et al., 2021). Other cannabinoids, such as cannabichromene (CBC), cannabinol (CBN), and cannabigerol (CBG), also exhibited MICs between 1 and 2 µg/mL against *S. aureus* strains (Werner et al., 2024). However, efficacy against Gram-negative bacteria is generally lower, with MICs and minimum lethal concentrations (MLCs) often exceeding 3000 µM for *Escherichia coli* and *Pseudomonas aeruginosa* (Luz-Veiga et al., 2023). These findings highlight the potential of CSL and its compounds as a source of novel antimicrobial agents, particularly against resistant Gram-positive pathogens.

Table 4
Minimum inhibitory concentration (MIC) and minimum bactericidal concentration (MBC) of the MeOH extract obtained from the flowers, stems and leaves of *Cannabis sativa* L. (CSL).

No.	Sample	*Escherichia coli* ATCC11775		*Staphylococcus aureus* ATCC12600	
		MIC (mg/mL)	MBC (mg/mL)	MIC (µg/mL)	MBC (µg/mL)
1	Flower	16	16	0.03*	15.6*
2	Leaf	32	32	0.06*	62.5*
3	Stem	32	32	8	64

*The MIC and MBC results for the two samples (flower and leaf) against *Staphylococcus aureus* are expressed in µg/mL, whereas all other results are in mg/mL.

3.2.2. Results of antifungal assay for CSL extracts

The MIC and minimum fungicidal concentration (MFC) for the aerial parts of CSL against *Candida albicans* were determined to be consistent with the numerical values found for the corresponding antibacterial activities. The MIC for the flower, leaf, and stem extracts was 4 mg/mL, while the MFC was 16 mg/mL. Notably, the MIC of CSL aerial parts was four times lower—and thus more effective—than the relevant MFC. CSL extracts have also demonstrated antifungal properties, with MICs ranging from 200 to 400 µM against *Candida albicans* (Luz-Veiga et al., 2023).

3.3. Characterization of the silver nanoparticles (AgNPs) using MECS

For comprehensive characterization of silver nanoparticle synthesis and to determine the functional groups, the type of crystal lattice, size, elemental analysis and morphology of nanoparticles, FTIR, XRD, EDX and TEM devices were used.

3.3.1. The FT-IR spectrum analysis of synthesized AgNPs using MECS

The Fourier-transform infrared (FT-IR) spectroscopy technique is a qualitative method used to identify nanoparticles. The presence of absorption bands at specific wavenumbers offers valuable information about metallic nanoparticles (Chandraker et al., 2021; Eid, 2022). In this context, if nanoparticles are formed as metal oxides, peaks between 400 and 800 cm^{-1} correspond to metal-oxygen bonds (Kannan and Sundrarajan, 2015). Furthermore, peaks in other regions are associated with various bonds in organic compounds found in the plant extract that bind to the nanoparticles (Huang et al., 2007).

AgNPs synthesized using plant extracts can form through the adsorption of phytochemicals onto their surfaces via π-electron transfer, even in the absence of other strong binding agents (Huang et al., 2019). The FT-IR spectrum of AgNPs prepared with MECS is shown in Fig. 4. As observed, all absorption bands present in the plant extract are visible in this spectrum, although some may have shifted slightly. The FTIR spectrum of the AgNPs exhibited peaks at 478 and 800 cm^{-1}, which were attributed to Ag-O stretching vibrations and out-of-plane C-H bending vibrations of aromatic compounds, respectively (Mandal et al., 2021). Bands appearing at 1315, 1076-1640, and 2850 cm^{-1} were assigned to C-O, C=C, C=O, C-H, and O-H stretching vibrations of organic compounds from the plant extract. These results confirm the successful synthesis of AgNPs using CSL extract and provide insights into their composition and structure.

In several related studies, FT-IR analysis of AgNPs synthesized using CSL extracts reveals significant shifts in peak positions and intensities, indicating the involvement of various functional groups in the

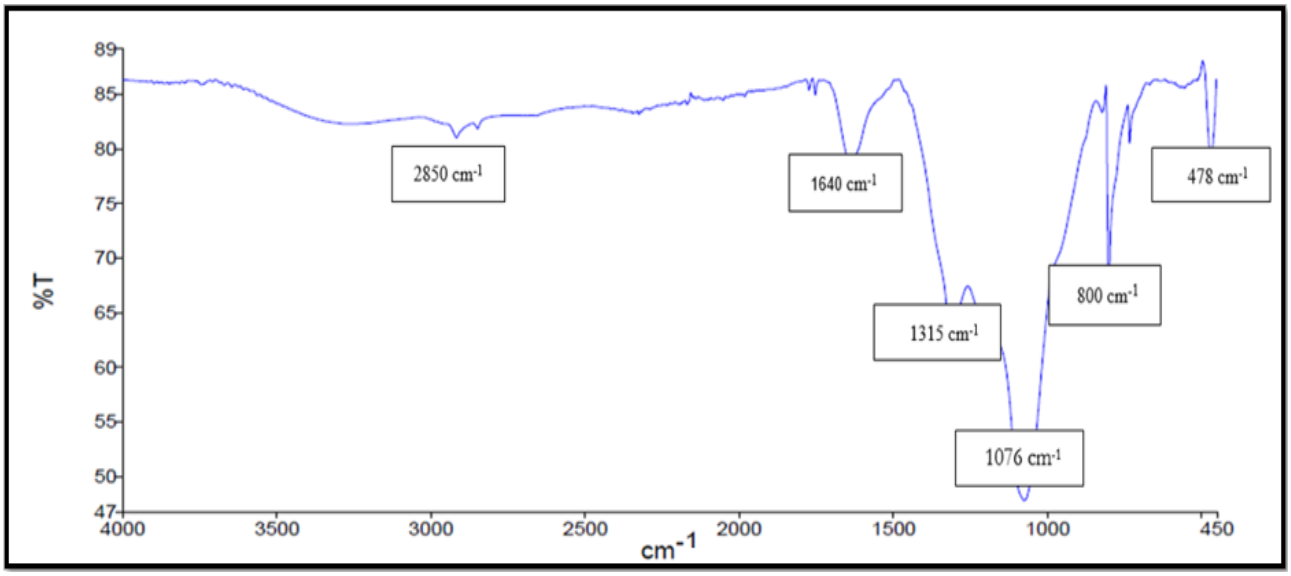

Fig. 4. Infrared spectrum of silver nanoparticles synthesized using *Cannabis satvia* L. extract.

reduction and stabilization processes. The FT-IR spectra of CSL root extract and biosynthesized AgNPs show distinct changes, particularly in the regions corresponding to hydroxyl and carbonyl groups (Ahmed and Ikram, 2015; Suman et al., 2022). Furthermore, for CSL-mediated AgNP synthesis, characteristic peaks are observed in the following ranges: 3200-3600 cm^{-1}, attributed to O-H and NH_2 stretching vibrations; 2925-2932 cm^{-1}, corresponding to C-H stretching; 1614-1621 cm^{-1}, representing N-H bending from glycoside compounds (Wan Mat Khalir et al., 2020); and 1516-1522 cm^{-1}, associated with the aromatic ring of terpenoid structures (Wan Mat Khalir et al., 2020).

The biosynthesis process typically results in peak shifts, changes in intensity and the appearance or disappearance of certain spectral bands. For example, peaks at 3399, 2932, 1522, and 530 cm^{-1} in the CSL extract shift to 3402, 2925, 1516, and 521 cm^{-1} in the AgNPs, respectively (Wan Mat Khalir et al., 2020). These shifts suggest the involvement of O-H, NH_2, C=O, and -C-H functional groups in the reduction and stabilization of AgNPs. Notably, the emergence of a new peak around 1829 cm^{-1} in the AgNP spectrum indicates the presence of carboxylate and C=C groups derived from terpenoid saponin structures, confirming the oxidation of glucose to gluconic acid (Wan Mat Khalir et al., 2020). The disappearance of peaks at 1445 and 1258 cm^{-1} further supports the binding mechanism between AgNPs and the components of the CSL extract (Wan Mat Khalir et al., 2020).

Compared to other plant extracts, CSL demonstrates efficient AgNP synthesis, with reactions typically completing within five minutes and producing nanoparticles with an average diameter of 12 nm (Ahmadi and Lackner, 2024). This rapid synthesis indicates that the CSL extract contains highly effective reducing agents for the conversion of silver ions.

3.3.2. Energy dispersive X-ray (EDX) spectroscopy analysis of synthesized AgNPs using MECS

Energy dispersive X-ray spectroscopy (EDX) is a qualitative technique used for identifying the elemental composition of nanoparticles (Ali et al., 2023; Ranjan et al., 2023). EDX was used to analyze the elemental composition of AgNPs synthesized with CSL extract, revealing peaks for silver, oxygen, and carbon that indicate plant extract components are attached to the nanoparticle surface (Fig. 5). In this context, the signals at 3.02 and 3.19 keV correspond to Ag Lα and Ag Lβ, respectively. Additionally, signals around 0.3 and 0.5 keV can be attributed to carbon and nitrogen elements, with the nitrogen component related to alkaloid compounds. The EDX spectroscopy indicates the percentage compositions of carbon (25.75%), nitrogen (69.4%), and silver (4.85%). Carbon and nitrogen are observed in the region below 1 keV, while silver is detected between 0.3 and 3.4 keV.

Our findings align with previous results documented in the literature. The EDX analysis of AgNPs synthesized using various plant methanol extracts typically reveals a strong peak at approximately 3 keV, confirming the presence of elemental silver (Bashir and Qureshi, 2015; Rajeshkumar et al., 2017). Additional peaks for carbon, oxygen, and other trace elements are often observed, indicating the presence of organic compounds from the plant extracts that may serve as capping agents (Bawazeer, 2024). The EDX spectra generally demonstrate a high purity of the synthesized AgNPs, with silver content varying based on the specific plant extract used (Goudarzi et al., 2016).

3.3.3. X-ray diffraction (XRD) analysis of synthesized AgNPs using MECS

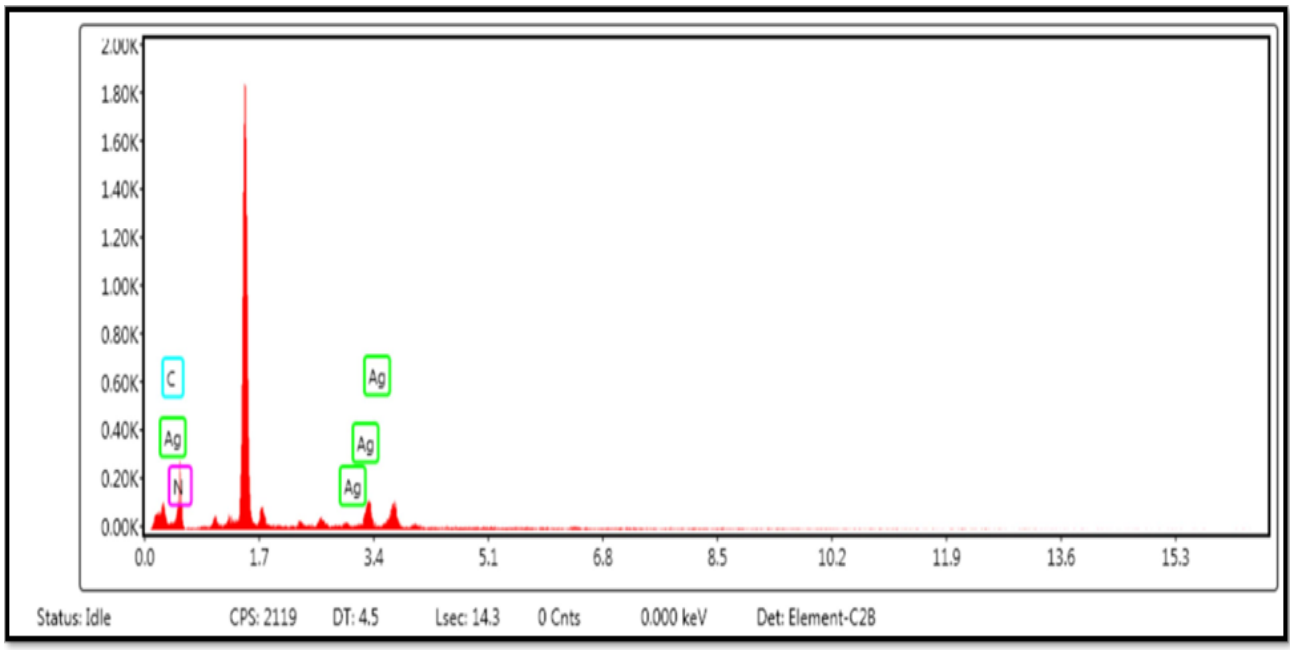

Fig. 5. Energy-dispersive X-ray spectroscopy (EDX) spectrum of synthetic silver nanoparticles using *Cannabis satvia* L. extract.

In this study, XRD was used to determine and confirm the crystalline structure of the synthesized nanoparticles. Following the green synthesis of AgNPs in the presence of MECS, the nanoparticles underwent XRD analysis for final confirmation. The XRD pattern of the synthesized nanoparticles using MECS is presented in Fig. 6, which aligns perfectly with the standard reference pattern (JCPDS card 04–0783) for metallic silver particles (Xu et al., 2006; Sarkar and Das, 2018). The observed signals at 37.455°, 44.115°, 64.185°, and 77.055° correspond to the (111), (200), (220), and (311) planes of the metallic AgNPs synthesized with MECS, respectively. Additionally, the broadening of the diffraction peaks suggests a small crystalline size of the AgNPs. The XRD analysis of AgNPs synthesized using various plant methanol extracts typically reveals face-centered cubic crystalline structures, with characteristic diffraction peaks at 2θ values of approximately 38°, 44°, 64°, and 77°, corresponding to the (111), (200), (220), and (311) planes of silver crystals (Jemal et al., 2017; Asif et al., 2022; Giri et al., 2022).

3.3.3.1. Determination of the size of synthesized AgNPs using MECS the Debye-Scherrer equation

According to the Debye-Scherrer equation (Eqn. 2), the size of nanoparticles can be determined from their XRD pattern.

$$D = K\lambda/\beta Cos\theta \quad \text{(Eqn. 2)}$$

In this equation, the parameters D, K, λ, β, and θ represent the nanoparticle size (in nanometers), a constant related to particle morphology (typically 0.9), the wavelength of the incident radiation from the source (CuKα) (0.154 nm), the full width at half maximum (FWHM) of the peak in radians and the diffraction angle, respectively. Using the Debye-Scherrer equation, the average crystallite size was calculated to be 30.03 nm.

In several previously reported studies, the Debye-Scherrer equation was employed to calculate the average crystallite size of AgNPs synthesized using various plant methanol extracts. The obtained results typically indicated crystallite sizes ranging from 5 to 50 nm, depending on the specific plant extract utilized (Kurapati and Srivastava, 2018; Santhoshkumar et al., 2021; Urnukhsaikhan et al., 2021). Notably, AgNPs synthesized with *Moringa oleifera* leaf extract exhibited an average crystallite size of 18 nm (Asif et al., 2022), while those produced using *Triumfetta rotundifolia* plant extract measured approximately 17 nm (Ananthi et al., 2016).

3.4. TEM images of the synthesized AgNPs using MECS

As can be seen from the TEM images in Fig. 7, the synthesized nanoparticles exhibit a quasi-spherical morphology with an average size of 50 nm and the particle size distribution ranges from 50 to 100 nm. These images also reveal the aggregation of nanoparticles (clumping), which is a common phenomenon in the synthesis of metal nanoparticles using plant extracts (Iravani, 2011; Mittal et al., 2013).

Similar to our findings, TEM images of AgNPs synthesized using various plant methanol extracts typically reveal spherical or quasi-spherical morphologies, with sizes ranging from 5 to 50 nm. For instance, TEM analysis of AgNPs synthesized using *Eugenia roxburghii* DC.

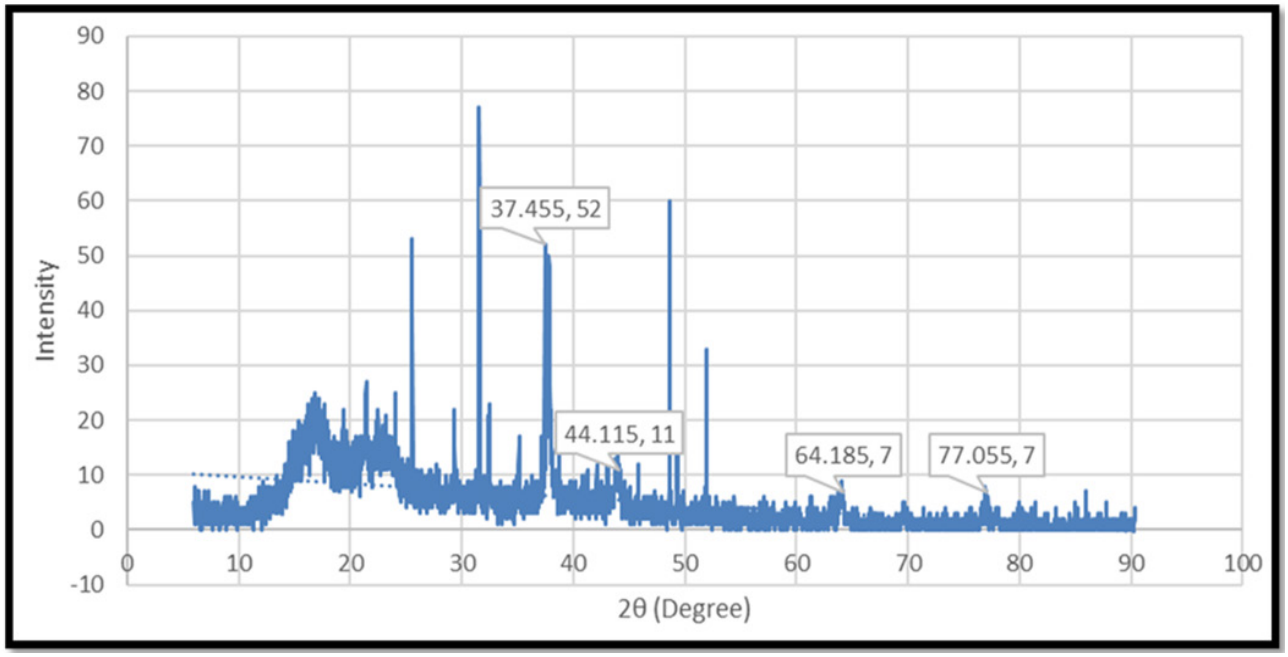

Fig. 6. X-ray diffraction (XRD) pattern of synthetic silver nanoparticles using *Cannabis satvia* L. extract.

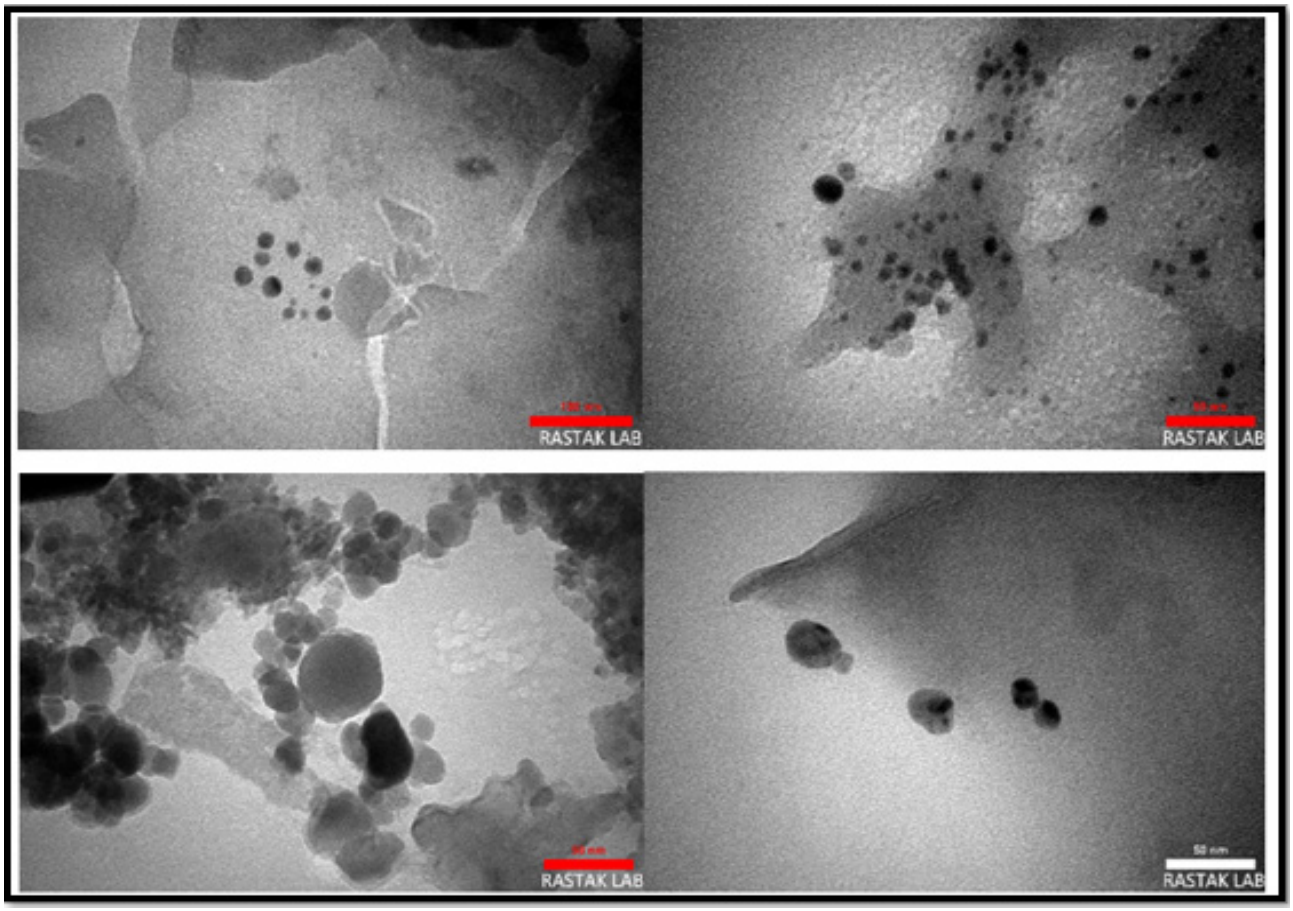

Fig. 7. Transmission electron microscopy (TEM) images of silver nanoparticles synthesized by *Cannabis satvia* L.

leaf extract showed particle sizes between 25 and 50 nm (Giri et al., 2022). Similarly, AgNPs produced from *Leucas aspera* and *Hyptis suaveolens* extracts exhibited spherical shapes with average sizes of 18 and 17 nm, respectively (Elumalai et al., 2017). TEM images of AgNPs synthesized using coffee and tea leaf extracts

at room temperature demonstrated the formation of well-dispersed nanoparticles (Santra et al., 2014). The morphology and size distribution of the nanoparticles can vary depending on the specific plant extract used, with some studies reporting the presence of aggregates or clusters (Kim et al., 2023). These variations in size and morphology are attributed to the different reducing and capping agents present in the plant extracts, which influence the nucleation and growth processes of the nanoparticles (Goudarzi et al., 2016; Stozhko et al., 2024).

4. Concluding remarks

This study provides new insights into the green synthesis of AgNPs using methanolic extracts of CSL, showcasing its dual role as a natural reducing and capping agent. The biological evaluation of the extracts revealed moderate antioxidant, antibacterial, and antifungal activities. The characterization results confirmed the formation of stable nanoparticles with well-defined crystalline structures, indicating the success of this green synthesis approach. Compared to the traditional chemical synthesis methods, the use of plant-based extracts ensures sustainability, safety, and cost-effectiveness by minimizing the use of toxic chemicals.

Despite the promising outcomes, future studies must address several limitations. First, the precise mechanism of nanoparticle formation using CSL extracts remains unclear and requires further investigation. Understanding the roles of individual bioactive compounds in reducing and stabilizing the nanoparticles could help optimize the synthesis process. Additionally, the stability and scalability of the synthesized nanoparticles are crucial factors for industrial applications that need to be thoroughly explored. Current work is limited to *in vitro* assays; therefore, comprehensive *in vivo* studies are necessary to assess the biosafety, pharmacokinetics and therapeutic potential of the nanoparticles in living systems.

Future research should focus on expanding the scope of biological activities, particularly in cancer therapy, wound healing, and drug delivery systems. The synergistic effects between plant-derived bioactive compounds and AgNPs may open new avenues for developing multifunctional nanomaterials with enhanced efficacy. Furthermore, integrating advanced synthesis techniques, such as microwave or ultrasound-assisted methods, could improve the yield, size control, and homogeneity of nanoparticles. The development of nanoparticle-based formulations for targeted delivery and controlled release systems could significantly enhance their biomedical utility.

In conclusion, this study underscores the potential of CSL as a versatile resource for green nanotechnology. With continued research, plant-mediated nanoparticle synthesis could pave the way for sustainable and innovative solutions in nanomedicine, agriculture, and environmental remediation. This work contributes to the expanding body of knowledge on eco-friendly nanomaterials and emphasizes the significance of interdisciplinary approaches in realizing their full potential for scientific and industrial advancements.

Abbreviations

AgNPs: Silver nanoparticles; **BHT:** Butylated hydroxytoluene; **CBC:** Cannabichromene; **CBG:** Cannabigerol; **CBN:** Cannabinol; **DPPH:** 1,1-Diphenyl-2-picrylhydrazyl; **DMSO:** Dimethyl sulfoxide; **EDX:** Energy-dispersive X-ray spectroscopy; **FDA:** Food and Drug Administration; **FWHM:** Full width at half maximum; **FT-IR:** Fourier-transform infrared spectroscopy; **GA:** Gallic acid; **IC_{50}:** Inhibitory concentration; **IR:** Infrared; **MLCs:** Minimum lethal concentrations; **MFC:** Minimum fungicidal concentration; **MRSA:** Methicillin-resistant *S. aureus*; **PKS:** Polyketide synthase; **RSA:** Radical scavenging activity; **Ru:** Rutin; **SEM:** Scanning electron microscopy; **SPR:** Surface plasmon resonance; **TEM:** Transmission electron microscopy; **TFC:** Total flavonoid content; **TPC:** Total phenolic content; **XRD:** X-ray diffraction.

Acknowledgment

The authors would like to express their sincere gratitude to Department of Chemistry and Biochemistry, Sha.C., Islamic Azad Uni-versity, Shahrood, for providing the financial support and research facilities required for conducting this study. The technical assistance and access to laboratory equipment and analytical instruments were crucial to the successful completion of this work. This valuable support is deeply appreciated and has significantly contributed to the advancement of this research

Author contribution statement

Conceptualization and literature search were performed by Majid Mohammadhosseini and Behnam Mahdavi. The first and final drafts of the manuscript were prepared by Mohammad Reza Kianasab and Majid Mohammadhosseini. Majid Mohammadhosseini and Behnam Mahdavi critically analyzed and gave suggestions to finalize the manuscript. All authors read and approved the final manuscript.

Conflict of interest

The authors declare that there is no conflict of interest.

References

Ahidar, N., Labhar, A., Benamari, O., Ahari, M., Salhi, A., Elyoussfi, A., Amhamdi, H., 2024. Phenolic content and antioxidant activity of *Cannabis sativa* L. flowers from the Ketama region in Northern Morocco. Ecol. Eng. Environ. Tech. 25(1), 209-215.

Ahmadi, F., Lackner, M., 2024. Green synthesis of silver nanoparticles from *Cannabis sativa*: Properties, synthesis, mechanistic aspects, and applications.

ChemEngineering 8(4), 64.
Ahmed, M., Ji, M., Qin, P., Gu, Z., Liu, Y., Sikandar, A., Iqbal, M.F., Javeed, A., 2019. Phytochemical screening, total phenolic and flavonoids contents and antioxidant activities of *Citrullus colocynthis* L. and *Cannabis sativa* L. Appl. Ecol. Environ. Res. 17(3), 6961-6979.
Ahmed, S., Ikram, S., 2015. Silver nanoparticles: One pot green synthesis using *Terminalia arjuna* extract for biological application. J. Nanomed. Nanotechnol. 6(4), 1-6.
Ali, M.H., Azad, M.A.K., Khan, K.A., Rahman, M.O., Chakma, U., Kumer, A., 2023. Analysis of crystallographic structures and properties of silver nanoparticles synthesized using PKL extract and nanoscale characterization techniques. ACS Omega 8(31), 28133-28142.
Amalia, N., Okta, F.N., Zahra, A.A., Nuari, D.A., 2024. Update review: Extraction, purification, and pharmacological activities of Gotu Kola terpenoids. Lett. Appl. NanoBioSci. 13(1), 1-17.
Ananthi, P., Jeyapaul, U., Anand, A.J.B., Kala, S.M.J., 2016. Green synthesis and characterization of silver nanoparticles using *Triumfetta rotundifolia* plant extract and its antibacterial activities. J. Nat. Prod. Plant Resour. 6(3), 21-27.
Arabkhani, P., Asfaram, A., Aghaei-Jazeh, M., Ateia, M., 2022. Plant-mediated green synthesis of nanocomposite-based multifunctional adsorbent with antibacterial activity and high removal efficiency of micropollutants from contaminated waters. J. Water Process Eng. 49, 103025.
Arora, R., Babbar, R., Kaur, R., Rana, P., 2023. An Insight into the Potential of Natural Products as Anti-inflammatory Agents A Systematic Review, Manufacturing Technologies and Production Systems: Principles and Practices. CRC Press, pp. 152-162.
Asif, M., Yasmin, R., Asif, R., Ambreen, A., Mustafa, M., Umbreen, S., 2022. Green synthesis of silver nanoparticles (AgNPs), structural characterization, and their antibacterial potential. Dose Response 20(2), 15593258221088709.
Banerjee, R., Erridge, S., Salazar, O., Mangal, N., Couch, D., Pacchetti, B., Sodergren, M.H., 2022. Real world evidence in medical *Cannabis* research. Ther. Innov. Regul. Sci. 56(1), 8-14.
Bashir, T., Qureshi, M.Z., 2015. Phytosynthesis of silver nanoparticles using *E. camaldulensis* leaf extract and their characterization. J. Chil. Chem. Soc. 60(1), 2861-2863.
Bautista, J.L., Yu, S., Tian, L., 2021. Flavonoids in *Cannabis sativa*: Biosynthesis, bioactivities, and biotechnology. ACS Omega 6(8), 5119-5123.
Bawazeer, S., 2024. Green synthesis of silver nanoparticles from *Euphorbia milii* plant extract for enhanced antibacterial and enzyme inhibition effects. Int. J. Health Sci. 18(2), 25.
Bawazeer, S., Rauf, A., Rahman, K.U., Ali, J., Uddin, G., Begum, F., Mubarak, M.S., Ramadan, M.F., 2020. Green synthesis and antimicrobial potential of silver/gold nanoparticles functionalized with *Debregeasia salicifolia* D. Don. J. Pure Appl. Microbiol. 14(4), 2513-2523.
Blainski, A., Lopes, G.C., De Mello, J.C.P., 2013. Application and analysis of the Folin Ciocalteu method for the determination of the total phenolic content from *Limonium brasiliense* L. Molecules 18(6), 6852-6865.
Blaskovich, M.A.T., Kavanagh, A.M., Elliott, A.G., Zhang, B., Ramu, S., Amado, M., Lowe, G.J., Hinton, A.O., Pham, D.M.T., Zuegg, J., Beare, N., Quach, D., Sharp, M.D., Pogliano, J., Rogers, A.P., Lyras, D., Tan, L., West, N.P., Crawford, D.W., Peterson, M.L., Callahan, M., Thurn, M., 2021. The antimicrobial potential of cannabidiol. Commun. Biolog. 4(1), 7.
Bowe, A., Kerr, P.L., 2024. Endogenous Opioid Activity as the Mechanism of Action for *Mitragyna speciosa* (Kratom): The Current State of the Evidence, Advances in Neurobiology. Springer, pp. 287-313.
Bukowska, B., 2024. Current and potential use of biologically active compounds derived from *Cannabis sativa* L. in the treatment of selected diseases. Int. J. Mol. Sci. 25(23), 12738.
Cásedas, G., Moliner, C., Maggi, F., Mazzara, E., López, V., 2022. Evaluation of two different *Cannabis sativa* L. extracts as antioxidant and neuroprotective agents. Front. Pharmacol. 13, 1009868.
Chandra, S., Khan, S., Avula, B., Lata, H., Yang, M.H., Elsohly, M.A., Khan, I.A., 2014. Assessment of total phenolic and flavonoid content, antioxidant properties, and yield of aeroponically and conventionally grown leafy vegetables and fruit crops: A comparative study. Evid. Based Complement. Alternat. Med. 2014, 253875.
Chandraker, S.K., Ghosh, M.K., Lal, M., Shukla, R., 2021. A review on plant-mediated synthesis of silver nanoparticles, their characterization and applications. Nano. Express. 2(2), 022008.
Chen, L., Li, H.L., Zhou, H.J., Zhang, G.Z., Zhang, Y., Wang, Y.M., Wang, M.Y., Yang, H., Gao, W., 2024. Feature-based molecular network-assisted cannabinoid and flavonoid profiling of *Cannabis sativa* leaves and their antioxidant properties. Antioxidants 13(6), 749.
Coronado-Aceves, E.W., Sánchez-Escalante, J.J., López-Cervantes, J., Robles-Zepeda, R.E., Velázquez, C., Sánchez-Machado, D.I., Garibay-Escobar, A., 2016. Antimycobacterial activity of medicinal plants used by the Mayo people of Sonora, Mexico. J. Ethnopharmacol. 190, 106-115.
Demarchi, C.A., Cruz, A.B., da Silva Bitencourt, C.M., Farias, I.V., Ślawska-Waniewska, A., Nedelko, N., Dłużewski, P., Morawiec, K., Calisto, J.F.F., Martello, R., Dal Magro, J., Rodrigues, C.A., 2020. *Eugenia umbelliflora* mediated reduction of silver nanoparticles incorporated into *O*-carboxymethylchitosan/γ-Fe_2O_3: Synthesis, antimicrobial activity and toxicity. Int. J. Biol. Macromol. 155, 614-624.
Eid, M.M., 2022. Characterization of Nanoparticles by FTIR and FTIR-Microscopy, Handbook of Consumer Nanoproducts. Springer Nature, pp. 645-673.
Elumalai, D., Hemavathi, M., Deepaa, C.V., Kaleena, P.K., 2017. Evaluation of phytosynthesised silver nanoparticles from leaf extracts of *Leucas aspera* and *Hyptis suaveolens* and their larvicidal activity against malaria, dengue and filariasis vectors. Parasite Epidemiol. Control 2(4), 15-26.
Flores-Sanchez, I.J., Verpoorte, R., 2008. PKS activities

and biosynthesis of cannabinoids and flavonoids in *Cannabis sativa* L. plants. Plant Cell Physiol. 49(12), 1767-1782.
Fordjour, E., Manful, C.F., Sey, A.A., Javed, R., Pham, T.H., Thomas, R., Cheema, M., 2023. *Cannabis*: A multifaceted plant with endless potentials. Front. Pharmacol. 14, 1200269.
Giardina, A., Palmieri, R., Ponticelli, M., Antonelli, C., Carlucci, V., Colangelo, M., Benedetto, N., Di Fazio, A., Milella, L., 2024. Is a low dosage of medical *Cannabis* effective for treating pain related to fibromyalgia? A pilot study and systematic review. J. Clin. Med. 13(14), 4088.
Giri, A.K., Jena, B., Biswal, B., Pradhan, A.K., Arakha, M., Acharya, S., Acharya, L., 2022. Green synthesis and characterization of silver nanoparticles using *Eugenia roxburghii* DC. extract and activity against biofilm-producing bacteria. Sci. Rep. 12(1), 8383.
Goudarzi, M., Mir, N., Mousavi-Kamazani, M., Bagheri, S., Salavati-Niasari, M., 2016. Biosynthesis and characterization of silver nanoparticles prepared from two novel natural precursors by facile thermal decomposition methods. Sci. Rep. 6(1), 32539.
Gulcin, İ., Alwasel, S.H., 2023. DPPH radical scavenging assay. Process. 11(8), 2248.
Hourfane, S., Mechqoq, H., Bekkali, A.Y., Rocha, J.M., El Aouad, N., 2023. A comprehensive review on *Cannabis sativa* ethnobotany, phytochemistry, molecular docking and biological activities. Plants 12(6), 1245.
Huang, J., Li, Q., Sun, D., Lu, Y., Su, Y., Yang, X., Wang, H., Wang, Y., Shao, W., He, N., Hong, J., Chen, C., 2007. Biosynthesis of silver and gold nanoparticles by novel sundried *Cinnamomum camphora* leaf. Nanotechnology 18(10), 105104.
Huang, M., Liu, S., Gong, S., Xu, P., Yang, K., Chen, S., Wang, C., Chen, Q., 2019. Silver nanoparticles encapsulated in an N-doped porous carbon matrix as high-active catalysts toward oxygen reduction reaction via electron transfer to outer graphene shells. ACS Sustainable Chem. Eng. 7(19), 16511-16519.
Iravani, S., 2011. Green synthesis of metal nanoparticles using plants. Green Chem. 13(10), 2638-2650.
Izzo, L., Castaldo, L., Narváez, A., Graziani, G., Gaspari, A., Rodríguez-Carrasco, Y., Ritieni, A., 2020. Analysis of phenolic compounds in commercial *Cannabis sativa* L. inflorescences using UHPLC-Q-orbitrap HRMs. Molecules 25(3), 631.
Jemal, K., Sandeep, B.V., Pola, S., 2017. Synthesis, characterization, and evaluation of the antibacterial activity of *Allophylus serratus* leaf and leaf derived callus extracts mediated silver nanoparticles. J. Nanomater. 2017(1), 4213275.
Jin, D., Dai, K., Xie, Z., Chen, J., 2020. Secondary metabolites profiled in *Cannabis* inflorescences, leaves, stem barks, and roots for medicinal purposes. Sci. Rep. 10(1), 3309.
Kalinowska, M., Płońska, A., Trusiak, M., Gołębiewska, E., Gorlewska-Pietluszenko, A., 2022. Comparing the extraction methods, chemical composition, phenolic contents and antioxidant activity of edible oils from *Cannabis sativa* and *Silybum marianu* seeds. Sci. Rep. 12(1), 20609.
Kannan, S.K., Sundrarajan, M., 2015. Green synthesis of ruthenium oxide nanoparticles: Characterization and its antibacterial activity. Adv. Powder Technol. 26(6), 1505-1511.
Kianasab, M.R., Mohammadhosseini, M., Nekoei, M., Mahdavi, B., Baheri, T., 2023. GC/MS analysis of the hydrodistilled essential oils and volatiles from the aerial parts of *Cannabis sativa* L. Nat. Prod. Res., 1-5.
Kim, S.M., Choi, H.J., Lim, J.A., Woo, M.A., Chang, H.J., Lee, N., Lim, M.C., 2023. Biosynthesis of silver nanoparticles from *Duchesnea indica* extracts using different solvents and their antibacterial activity. Microorganisms 11(6), 1539.
Kosiba, J.D., Maisto, S.A., Ditre, J.W., 2019. Patient-reported use of medical *Cannabis* for pain, anxiety, and depression symptoms: Systematic review and meta-analysis. Soc. Sci. Med. 233, 181-192.
Kurapati, S., Srivastava, P., 2018. Application of Debye-Scherrer formula in the determination of silver nano particles shape. Int. J. Manag. Technol. Eng. 8(7), 81-84.
Lapierre, É., Monthony, A.S., Torkamaneh, D., 2023. Genomics-based taxonomy to clarify *Cannabis* classification. Genome 66(08), 202-211.
Lawag, I.L., Nolden, E.S., Schaper, A.A.M., Lim, L.Y., Locher, C., 2023. A modified Folin-Ciocalteu assay for the determination of total phenolics content in honey. Appl. Sci. 13(4), 2135.
Leinen, Z.J., Mohan, R., Premadasa, L.S., Acharya, A., Mohan, M., Byrareddy, S.N., 2023. Therapeutic potential of *Cannabis*: A comprehensive review of current and future applications. Biomedicines 11(10), 2630.
Lentz, D.L., Hamilton, T.L., Meyers, S.A., Dunning, N.P., Reese-Taylor, K., Hernández, A.A., Walker, D.S., Tepe, E.J., Esquivel, A.F., Weiss, A.A., 2024. Psychoactive and other ceremonial plants from a 2,000-year-old Maya ritual deposit at Yaxnohcah, Mexico. PLOS ONE 19(4), e0301497.
Li, M., Qian, M., Jiang, Q., Tan, B., Yin, Y., Han, X., 2023. Evidence of flavonoids on disease prevention. Antioxidants 12(2), 527.
Liu, Y., Xiao, A.P., Cheng, H., Liu, L.L., Kong, K.W., Liu, H.Y., Wu, D.T., Li, H.B., Gan, R.Y., 2022. Phytochemical differences of hemp (*Cannabis sativa* L.) leaves from different germplasms and their regulatory effects on lipopolysaccharide-induced inflammation in Matin-Darby canine kidney cell lines. Front. Nutr. 9, 902625.
Luz-Veiga, M., Amorim, M., Pinto-Ribeiro, I., Oliveira, A.L.S., Silva, S., Pimentel, L.L., Rodríguez-Alcalá, L.M., Madureira, R., Pintado, M., Azevedo-Silva, J., Fernandes, J., 2023. Cannabidiol and cannabigerol exert antimicrobial activity without compromising skin microbiota. Int. J. Mol. Sci. 24(3), 2389.
Mahdavi, B., Mohammadhosseini, M., 2022. Antioxidant, antimicrobial and anti-prostate cancer activity of the extracts from different parts of *Etlingera velutina* (Ridl.) R. M. Sm (Zingiberaceae). Trends Phytochem. Res. 6(4), 353-362.
Mandal, S., Marpu, S.B., Hughes, R., Omary, M.A., Shi, S.Q., 2021. Green synthesis of silver nanoparticles using *Cannabis sativa* extracts and their anti-bacterial activity.

Green Sustain. Chem. 11(1), 38-48.
Mathur, N.K., Ruhm, C.J., 2023. Marijuana legalization and opioid deaths. J. Health Econ. 88, 102728.
Matos, C., Pereira, A.T., Dias, M.J., Sousa, C., Vinha, A.F., Moutinho, C., Carvalho, M., 2025. *Cannabis* for chronic pain: Mechanistic insights and therapeutic challenges. Stresses 5(1), 7.
Meena, P.R., Singh, A.P., Tejavath, K.K., 2020. Biosynthesis of silver nanoparticles using *Cucumis prophetarum* aqueous leaf extract and their antibacterial and antiproliferative activity against cancer cell lines. ACS Omega 5(10), 5520-5528.
Mirzamohammad, E., Alirezalu, A., Alirezalu, K., Norozi, A., Ansari, A., 2021. Improvement of the antioxidant activity, phytochemicals, and cannabinoid compounds of *Cannabis sativa* by salicylic acid elicitor. Food Sci. Nutr. 9(12), 6873-6881.
Mishra, K., Ojha, H., Chaudhury, N.K., 2012. Estimation of antiradical properties of antioxidants using DPPH center dot assay: A critical review and results. Food Chem. 130(4), 1036-1043.
Mittal, A.K., Chisti, Y., Banerjee, U.C., 2013. Synthesis of metallic nanoparticles using plant extracts. Biotechnol. Adv. 31(2), 346-356.
Mohammadhosseini, M., Jeszka-Skowron, M., 2023. A systematic review on the ethnobotany, essential oils, bioactive compounds, and biological activities of *Tanacetum* species. Trends Phytochem. Res. 7(1), 1-29.
Moond, M., Singh, S., Sangwan, S., Rani, S., Beniwal, A., Rani, J., Kumari, A., Rani, I., Devi, P., 2023. Phytofabrication of silver nanoparticles using *Trigonella foenum-graceum* L. leaf and evaluation of its antimicrobial and antioxidant activities. Int. J. Mol. Sci. 24(4), 3480.
Motiejauskaitė, D., Ullah, S., Kundrotaitė, A., Žvirdauskienė, R., Bakšinskaitė, A., Barčauskaitė, K., 2023. Isolation of biologically active compounds from *Cannabis sativa* L. inflorescences by using different extraction solvents and evaluation of antimicrobial activity. Antioxidants 12(5), 998.
Murti, Y., Singh, S., Pathak, K., 2024. Classical Techniques for Extracting Essential Oils from Plants, Essential Oils: Extraction Methods and Applications. Wiley, pp. 795-858.
Ndlovu, S.B., Naidoo, D., van Staden, J., Gebashe, F.C., 2024. A systematic review of *Cannabis sativa* L. cultivation techniques: A comprehensive overview of tissue culture innovations and growth optimization. Ind. Crops Prod. 222, 119539.
Perlman, A.I., McLeod, H.M., Ventresca, E.C., Salinas, M.G., Post, P.J., Schuh, M.J., Abu Dabrh, A.M., 2021. Medical *Cannabis* state and federal regulations: Implications for United States health care entities. Mayo Clin. Proc. 96(10), 2671-2681.
Pradeep, M., Kruszka, D., Kachlicki, P., Mondal, D., Franklin, G., 2022. Uncovering the phytochemical basis and the mechanism of plant extract-mediated eco-friendly synthesis of silver nanoparticles using ultra-performance liquid chromatography coupled with a photodiode array and high-resolution mass spectrometry. ACS Sustainable Chem. Eng. 10(1), 562-571.
Rajasekar, A., Moorthi, M., Deivasigamani, P., Sekar, S., Amar, G., 2023. A Review on Screening, Isolation, and Characterization of Phytochemicals in Plant Materials: Methods and Techniques, Pharmacological Benefits of Natural Agents. IGI Global, pp. 1-12.
Rajeshkumar, S., Malarkodi, C., Kumar, V., 2017. Synthesis and characterization of silver nanoparticles from marine brown seaweed and its antifungal efficiency against clinical fungal pathogens. Asian J. Pharm. Clin. Res., 190-193.
Ramos, R., Bezerra, I., Ferreira, M., Soares, L., 2017. Spectrophotometric quantification of flavonoids in herbal material, crude extract, and fractions from leaves of *Eugenia uniflora* Linn. Pharmacogn. Res. 9(3), 253-260.
Ranjan, R., Kumar, M., Prasad, S.M., 2023. XRD analysis of nanoparticles synthesized using aqueous and alcoholic extracts of *Cuscuta reflexa*. Balneo. PRM. Res. J. 14(3), 585.
Ransing, R., de la Rosa, P.A., Pereira-Sanchez, V., Handuleh, J.I.M., Jerotic, S., Gupta, A.K., Karaliuniene, R., Filippis, R., Peyron, E., Güngör, E.S., Boujraf, S., Yee, A., Vahdani, B., Shoib, S., Stowe, M.J., Jaguga, F., Dannatt, L., Silva, A.K.D., Grandinetti, P., Jatchavala, C., 2022. Current state of *Cannabis* use, policies, and research across sixteen countries: Cross-country comparisons and international perspectives. Trends 44, e20210263.
Rehm, J., Elton-Marshall, T., Sornpaisarn, B., Manthey, J., 2019. Medical marijuana. What can we learn from the experiences in Canada, Germany and Thailand? Int. J. Drug Policy 74, 47-51.
Santhoshkumar, R., Hima Parvathy, A., Soniya, E.V., 2021. Phytosynthesis of silver nanoparticles from aqueous leaf extracts of *Piper colubrinum*: Characterisation and catalytic activity. J. Exp. Nanosci. 16(1), 295-309.
Santra, T.S., Tseng, F.-G.K., Barik, T.K., 2014. Biosynthesis of silver and gold nanoparticles for potential biomedical applications—A brief review. J. Nanopharm. Drug Deliv. 2(4), 249-265.
Sarkar, S., Das, R., 2018. Shape effect on the elastic properties of Ag nanocrystals. Micro Nano Lett. 13(3), 312-315.
Sharif, N., Jabeen, H., 2024. Natural sources for coumarins and their derivatives with relevance to health-promoting properties: A systematic review. Trends Phytochem. Res. 8(3), 149-162.
Shraim, A.M., Ahmed, T.A., Rahman, M.M., Hijji, Y.M., 2021. Determination of total flavonoid content by aluminum chloride assay: A critical evaluation. LWT 150, 111932.
Singh, A., Singh, D., Sharma, S., Mittal, N., 2023. A review on biosynthesis, regulation, and applications of terpenes and terpenoids. Trends Phytochem. Res. 7(4), 228-245.
Stasiłowicz-Krzemień, A., Sip, S., Szulc, P., Walkowiak, J., Cielecka-Piontek, J., 2023. The antioxidant and neuroprotective potential of leaves and inflorescences extracts of selected hemp varieties obtained with $scCO_2$. Antioxidants 12(10), 1827.
Steel, L., Welling, M., Ristevski, N., Johnson, K., Gendall, A., 2023. Comparative genomics of flowering behavior

in *Cannabis sativa*. Front. Plant Sci. 14, 1227898.
Stozhko, N., Tarasov, A., Tamoshenko, V., Bukharinova, M., Khamzina, E., Kolotygina, V., 2024. Green silver nanoparticles: Plant-extract-mediated synthesis, optical and electrochemical properties. Physchem. 4(4), 402-419.
Suman, S., Loveleen, L., Bhandari, M., Syed, A., Bahkali, A.H., Manchanda, R., Nimesh, S., 2022. Antibacterial, antioxidant, and haemolytic potential of silver nanoparticles biosynthesized using roots extract of *Cannabis sativa* plant. Artif. Cells Nanomed. Biotechnol. 50(1), 343-351.
Tiago, F.J., Paiva, A., Matias, A.A., Duarte, A.R.C., 2022. Extraction of bioactive compounds from *Cannabis sativa* L. flowers and/or leaves using deep eutectic solvents. Front. Nutr. 9, 892314.
Torres, C.A., Zampini, I.C., Nunez, M.B., Isla, M.I., Castro, M.P., Gonzalez, A.M., 2013. *In vitro* antimicrobial activity of 20 selected climber species from the Bignoniaceae family. Nat. Prod. Res. 27(22), 2144-2148.
Urnukhsaikhan, E., Bold, B.E., Gunbileg, A., Sukhbaatar, N., Mishig-Ochir, T., 2021. Antibacterial activity and characteristics of silver nanoparticles biosynthesized from *Carduus crispus*. Sci. Rep. 11(1), 21047.
Vanlalveni, C., Lallianrawna, S., Biswas, A., Selvaraj, M., Changmai, B., Rokhum, S.L., 2021. Green synthesis of silver nanoparticles using plant extracts and their antimicrobial activities: A review of recent literature. RSC Adv. 11(5), 2804-2837.
Velgosova, O., Dolinská, S., Podolská, H., Mačák, L., Čižmárová, E., 2024. Impact of plant extract phytochemicals on the synthesis of silver nanoparticles. Materials 17(10), 2252.
Wan Mat Khalir, W.K.A., Shameli, K., Jazayeri, S.D., Othman, N.A., Che Jusoh, N.W., Hassan, N.M., 2020. Biosynthesized silver nanoparticles by aqueous stem extract of *Entada spiralis* and screening of their biomedical activity. Front. Chem. 8, 620.
Werner, M., Bereswill, S., Heimesaat, M.M., 2024. A recent update on the antibacterial effects of distinct bioactive molecules derived from the *Cannabis* plant. Eur. J. Microbiol. Immunol. 14(4), 333-339.
Wilson, J., Langcake, A., Bryant, Z., Freeman, T.P., Leung, J., Chan, G.C., Englund, A., Graham, M., Stockings, E., 2025. The safety and efficacy of cannabinoids for the treatment of mental health and substance use disorders: Protocol for a systematic review and meta-analysis. Syst. Rev. 14(1), 1-12.
Wright, P., Walsh, Z., Margolese, S., Sanchez, T., Arlt, S., Belle-Isle, L., St.pierre, M., Bell, A., Daeninck, P., Gagnon, M., Lacasse, G., MacCallum, C., Mandarino, E., Yale, J., O'Hara, J., Costiniuk, C., 2020. Canadian clinical practice guidelines for the use of plant-based *Cannabis* and cannabinoid-based products in the management of chronic non-cancer pain and co-occurring conditions: Protocol for a systematic literature review. BMJ Open 10(5), e036114.
Xiang, G., Guo, S., Qin, J., Gao, H., Zhang, Y., Wang, S., 2024. Comprehensive insight into the pharmacology, pharmacokinetics, toxicity, detoxification and extraction of hypaconitine from *Aconitum* plants. J. Ethnopharmacol. 321, 117505.
Xu, J., Hu, J., Peng, C., Liu, H., Hu, Y., 2006. A simple approach to the synthesis of silver nanowires by hydrothermal process in the presence of gemini surfactant. J. Colloid Interface Sci. 298(2), 689-693.
Zhang, Y., Mahdavi, B., Mohammadhosseini, M., Rezaei-Seresht, E., Paydarfard, S., Qorbani, M., Karimian, M., Abbasi, N., Ghaneialvar, H., Karimi, E., 2021. Green synthesis of NiO nanoparticles using Calendula officinalis extract: Chemical charactrization, antioxidant, cytotoxicity, and anti-esophageal carcinoma properties. Arabian J. Chem. 14, 103105.